

AD 632140

FIELD OF  
AN AXIALLY SLOTTED CIRCULAR CYLINDER  
CLAD WITH AN INHOMOGENEOUS DIELECTRIC

BY  
GEORGE TYRAS

THE UNIVERSITY OF ARIZONA  
COLLEGE OF ENGINEERING  
ENGINEERING EXPERIMENT STATION  
TUCSON, ARIZONA

CONTRACT NO. AF 19(628) - 3834  
PROJECT NO. 4642  
TASK NO. 464202

SCIENTIFIC REPORT NO. 3

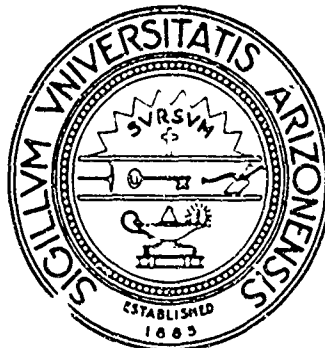
FEBRUARY 1966

CLEARINGHOUSE FOR FEDERAL SCIENTIFIC AND TECHNICAL INFORMATION		
Hardcopy	Microfilm	
\$ 2.60	.50	24 pp 2x
ARCHIVE COPY		

*code 1*

PREPARED FOR

AIR FORCE CAMBRIDGE RESEARCH LABORATORIES  
OFFICE OF AEROSPACE RESEARCH  
UNITED STATES AIR FORCE  
BEDFORD, MASSACHUSETTS



AFCLR-66-203

FIELD OF AN AXIALLY SLOTTED CIRCULAR CYLINDER  
CLAD WITH AN INHOMOGENEOUS DIELECTRIC

By

George Tyras

The University of Arizona  
College of Engineering  
Engineering Experiment Station  
Tucson, Arizona

Contract No. AF 19(628)-3834  
Project No. 4642  
Task No. 464202

Scientific Report No. 3  
February 1966

PREPARED FOR

Air Force Cambridge Research Laboratories  
Office of Aerospace Research  
United States Air Force  
Bedford, Massachusetts

Distribution of this document is unlimited.

TABLE OF CONTENTS

Abstract . . . . . 1

List of Contributors . . . . . ii

Related Contracts and Publications . . . . . ii

1. Introduction . . . . . 1

2. Theoretical Development . . . . . 3

    2.1 The Case  $p \neq -1$  . . . . . 7

    2.2 The Case  $p = -1$  . . . . . 10

3. Application to Small Cylinders . . . . . 11

4. Application to Large Cylinders . . . . . 12

    4.1 Integral Representation of the Solution . . . . . 13

    4.2 Fields in the Shadow Region . . . . . 13

    4.3 Fields in the Illuminated Region . . . . . 17

5. Numerical Results and Interpretation . . . . . 20

6. Figures . . . . . 22

7. Appendix . . . . . 29

8. References . . . . . 31

TABLE OF FIGURES

Fig. 1. Geometry of the problem . . . . .	22
Fig. 2. Inhomogeneous sheath profiles; (a) Increasing profile, .	23
(b) Decreasing profile . . . . .	24
Fig. 3. Variation of the radiation pattern as a function of the cylinder radius . . . . .	25
Fig. 4. Variation of the radiation pattern as a function of the inhomogeneity gradient . . . . .	26
Fig. 5. Variation of the radiation pattern as a function of the layer thickness . . . . .	27
Fig. 6. Ray focusing by the layer . . . . .	28

## ABSTRACT

The problem of an axial slot on a circular cylinder clad with a radially inhomogeneous plasma (dielectric) was considered recently by Rusch [1964]. Although his formulation is quite general inasmuch as it admits a realistic approximation to the plasma sheath inhomogeneities, the resulting solution is not well suited for computations of field patterns of large cylinders.

In the present formulation we consider the dielectric permittivity profile of the form  $\epsilon(\rho) = (\rho/b)^{2p}$ ,  $a \leq \rho \leq b$ , where 'a' is the radius of the conducting cylinder, 'b' is the outer radius of the dielectric coating and 'p' is an arbitrary parameter. It follows that the assumed profile is capable of representing an inhomogeneous cold plasma when  $p > 0$  and a real dielectric when  $p < 0$ . The apparent advantage of the present formulating is the fact that the wave equation can be solved in terms of known functions and the solution can be extended to large cylinders.

Field expressions appropriate to small and large cylinders are found using standard methods of harmonic series representation, Watson Transformation and saddle point integration. In the case of large cylinders coated with cold plasma, the radiation patterns are plotted for various combinations of the cylinder radius, thickness of the coating, and the inhomogeneity gradient. The radiation patterns are in good agreement with qualitative arguments of geometric optics.

### LIST OF CONTRIBUTORS

In addition to the author, Mr. Willard P. Webster and Mr. Udo Karst, graduate students in the Department of Electrical Engineering, contributed to the preparation of this report. Mr. Webster was responsible for the computer programming and numerical calculations and Mr. Karst prepared the illustrations.

### RELATED CONTRACTS AND PUBLICATIONS

The present report is a continuation of the research related to the plasma sheath effects on antennas. The previous publications are:

1. "An Experimental Study of Plasma Sheath Effects on Antennas" by G. Tyras, P. C. Bargeliotas, J. M. Hamm, and R. R. Schell, Scientific Report No. 1, AFCRL-65-53, Contract No. AF 19(628)-3834, December 1964.
2. "An Experimental Study of Plasma Sheath Effects on Antennas" by G. Tyras, P. C. Bargeliotas, J. M. Hamm, and R. R. Schell; Radio Science, J. Res. NBS/USNC-URSI, vol. 69D, No. 6, June 1965, pp. 839-850.
3. "Further Experimental Study of Plasma Sheath Effects on Antennas" by J. M. Hamm and G. Tyras, Scientific Report No. 2, AFCRL-65-608, Contract No. AF 19(628)-3834, July, 1965.

## 1. Introduction

The problem of a radiating slot on a dielectric clad cylinder occupies a relatively important position in microwave engineering. Its importance is due primarily to the phenomenon of a plasma sheath formed around a hypersonic vehicle during its reentry phase. Since the plasma can be represented under certain conditions by its equivalent dielectric permittivity, the problem of a plasma covered antenna can be reduced to one of a dielectric clad antenna that can be treated as a well-defined boundary value problem.

The boundary value problem approach to the plasma sheath phenomenon was used in the past by several authors. Tamir and Oliner [1962] and Omura [1962] obtained theoretical radiation patterns of a dielectric clad slot on a ground plane. Tyras et al [1965] obtained experimental confirmation of their results by means of an artificial plasma simulation technique. The problem of an axial slot on a circular cylinder clad with a dielectric layer was considered by Hasserjian [1965]. He formulated the solution in terms of an integral representation from which he was able to find the far field pertinent to a cylinder of a large radius.

The problem of a slot clad with inhomogeneous dielectric layer was attacked by two different methods. In the first method, the inhomogeneity of the layer was approximated by a series of discrete homogeneous and parallel layers [Hamm and Tyras, 1965; Harris and Pachares, 1965; Harris, 1965]. The resulting formulas are necessarily long and complicated but they can be programmed for a digital computer to obtain numerical results. In the case of cylindrical geometry, the formulas obtained by this method converge slowly when the radius of the cylinder is large and, consequently, their application is limited.

Another method of approach to the problem of inhomogeneities in the layer is that of a rigorous solution. Inasmuch as no general solution to the differential equation describing wave propagation in inhomogeneous regions exists, this approach suffers from the lack of versatility. However, Rusch [1964] found a solution to an inhomogeneous profile that allows, perhaps, the most realistic approximation to an inhomogeneous, continuously radially stratified plasma sheath. He chose a model of the dielectric permittivity profile of the form  $\epsilon(\rho) = A\rho^2 + B\rho + C$  where A, B, and C are arbitrary constant. The two linearly independent solutions of the wave equation are constructed using the well-known method of Frobenius. Consequently, his final expression for the fields appears as an infinite series that cannot be expressed in terms of known functions. When the radius of the cylinder is small, the resulting series converges well and numerical results can be obtained. When the radius of the cylinder is large, which is the case of great practical importance, the resulting series is slowly convergent and it is not suitable for numerical calculations.

In this paper we choose the dielectric permittivity profile of the form  $\epsilon(\rho) = (\rho/b)^{2p}$  where 'b' is the outer radius of the coating and 'p' is an arbitrary constant. This particular model admits exact solution of the pertinent differential equation in terms of Bessel functions. The model is capable of representing an increasing or decreasing profile when 'p' is positive or negative respectively. When 'p' is positive, this model can be related to the plasma frequency in the form  $(\omega_0/\omega)^2 = 1 - (\rho/b)^{2p}$ . It will follow that this representation will admit the specification of the plasma frequency,  $\omega_0$ , between the limits of the operating frequency and zero.



The principal advantage of the present formulation is the fact that the solution can be expressed in terms of known functions. After obtaining the familiar harmonic series representation, the integral representation can be found using the well-known Watson Transformation. The latter, in turn, enables obtaining the far field expression for an arbitrarily large cylinder which seems to be of some practical importance.

## 2. Theoretical Development

Consider an axially slotted cylinder clad with an concentric inhomogeneous layer of a dielectric that is a function of the radial variable only. The geometry of the problem is shown in Fig. 1. In the inhomogeneous dielectric region the fields must satisfy

$$\begin{aligned}\vec{\nabla} \times \vec{E}_1 &= i\omega\mu_0\vec{H}_1 \\ \vec{\nabla} \times \vec{H}_1 &= i\omega\epsilon_0\epsilon(\rho)\vec{E}_1 \\ E_{\phi 1}(a, \phi) &= \frac{V}{\Delta} \delta(\phi)\end{aligned}\quad (1)$$

where the harmonic time dependence of the form  $e^{-i\omega t}$  has been assumed and suppressed throughout. The excitation considered is of the form of an infinitely thin slot fed by a voltage  $V$  (delta function slot). In the free space region the fields must satisfy

$$\begin{aligned}\vec{\nabla} \times \vec{E}_0 &= i\omega\mu_0\vec{H}_0 \\ \vec{\nabla} \times \vec{H}_0 &= -i\omega\epsilon_0\vec{E}_0.\end{aligned}\quad (2)$$

Moreover, at the interface  $\rho = b$  the tangential components of the electric and the magnetic fields must be continuous which implies

$$H_{z1} = H_{z0}$$

$$E_{\phi 1} = E_{\phi 0} , \quad (3)$$

since the assumed geometry does not admit any other tangential field components.

Performing a curl operation on the second equation of (1) and substituting the first, one obtains a differential equation in terms of the magnetic field only, that is

$$\nabla^2 \vec{H}_1 + \frac{1}{\epsilon} \vec{\nabla} \epsilon \times \vec{\nabla} \times \vec{H}_1 + k_0^2 \epsilon \vec{H}_1 = 0 \quad (4)$$

where we used a well-known vector relation. The axial component of the vector equation (4) can be shown to be

$$\frac{1}{\rho} \frac{\partial}{\partial \rho} \left( \rho \frac{\partial H_{z1}}{\partial \rho} \right) + \frac{1}{\rho^2} \frac{\partial^2 H_{z1}}{\partial \phi^2} - \frac{1}{\epsilon} \left( \frac{\partial \epsilon}{\partial \rho} \frac{\partial H_{z1}}{\partial \rho} + \frac{1}{\rho^2} \frac{\partial \epsilon}{\partial \phi} \frac{\partial H_{z1}}{\partial \phi} \right) + k_0^2 \epsilon H_{z1} = 0 \quad (5)$$

which in the case that the dielectric permittivity is a function of the radial variable only becomes

$$\frac{1}{\rho} \frac{\partial}{\partial \rho} \left( \rho \frac{\partial H_{z1}}{\partial \rho} \right) - \frac{1}{\epsilon} \frac{\partial \epsilon}{\partial \rho} \frac{\partial H_{z1}}{\partial \rho} + \frac{1}{\rho^2} \frac{\partial^2 H_{z1}}{\partial \phi^2} + k_0^2 \epsilon H_{z1} = 0 . \quad (6)$$

Similarly, it can be shown that in the free space region the magnetic field must satisfy

$$\frac{1}{\rho} \frac{\partial}{\partial \rho} \left( \rho \frac{\partial H_{z0}}{\partial \rho} \right) + \frac{1}{\rho^2} \frac{\partial^2 H_{z0}}{\partial \phi^2} + k_0^2 H_{z0} = 0 . \quad (7)$$

It will be appropriate to seek the solution of the form

$$H_z(\rho, \phi) = \int_{-\infty}^{\infty} \psi_m(\rho) e^{im\phi} \quad (8)$$

from which it will follow that the radial functions  $\psi_{m1}(\rho)$  and  $\psi_{m0}(\rho)$  must satisfy the ordinary differential equations

$$\psi_{m1}'' + \left(\frac{1}{\rho} - \frac{\epsilon'}{\epsilon}\right) \psi_{m1}' + \left(k_o^2 \epsilon - \frac{m^2}{\rho^2}\right) \psi_{m1} = 0 \quad (9)$$

and

$$\psi_{m0}'' + \frac{1}{\rho} \psi_{m0}' + \left(k_o^2 - \frac{m^2}{\rho^2}\right) \psi_{m0} = 0 \quad (10)$$

where the denoted differentiations are with respect to  $\rho$ .

The further success in proceeding with the solution is contingent upon being able to solve the differential equation (9). Since a general solution for an arbitrary function  $\epsilon(\rho)$  is not known to exist, one must at this point specify the functional dependence of the dielectric permittivity,  $\epsilon$ . Rusch [1964] chose a model of the dielectric permittivity of the form  $\epsilon(\rho) = A\rho^2 + B\rho + C$  where  $A$ ,  $B$  and  $C$  are constants and found two linearly independent power series solutions to (9) using the method of Frobenius [Dettman, 1962]. His model is quite versatile inasmuch as it allows fairly realistic approximations to the electron density profile in a plasma sheath. The price paid for this is the complexity of the final solution which cannot be expressed in terms of known functions.

In this paper we shall choose the profile of the dielectric permittivity in the form

$$\epsilon(\rho) = \left(\frac{\rho}{b}\right)^{2p} \quad (11)$$

where 'b' is the outer radius of the coating and 'p' is an arbitrary number. In what follows we shall show that this particular choice of  $\epsilon(\rho)$  results in solutions to (9) in terms of known and tabulated functions.

The particular model of  $\epsilon(\rho)$  given in (11) is capable of representing an increasing profile when 'p' is positive and a decreasing profile when 'p' is negative. When 'p' is positive, this permittivity profile can be easily related to the electron density profile in a lossless, cold plasma via the relation

$$\frac{\omega_0}{\omega}^2 = 1 - \left(\frac{\rho}{b}\right)^{2p}$$

where  $\omega_0$  is the plasma frequency and  $(\omega_0/\omega)^2 = 8.06 \times 10^7 N/f^2$ , where N is the number of free electrons per cubic centimeter. The possible profiles of  $(\omega_0/\omega)^2$  versus  $\rho/b$  are shown in Fig. 2a. It will follow that the present representation will admit the specification of the plasma frequency  $\omega_0$  between the limits of the operating frequency  $\omega$  and zero. Once the plasma frequency is specified at the skin of the cylinder, however, the details of the profile are fixed. The latter restriction is not a serious one, however, inasmuch as it is known that the main contributions to the propagation characteristics will come from the bulk effect of the inhomogeneity rather than from the details of the permittivity profile [Liu and Wetzel, 1965].

When 'p' is negative then the assumed functional dependence for  $\epsilon(\rho)$  in (11) will represent a profile that decreases with an increasing radial distance as shown in Fig. 2b. This case is then applicable to the problem of a cylinder clad with real inhomogeneous dielectric.

When the form of  $\epsilon(\rho)$  given in (11) is substituted into (9), one obtains the differential equation

$$\psi_{m1}'' + \left(\frac{1-2p}{\rho}\right)\psi_{m1}' + \left(k_0^2 b^{-2p} \rho^{2p} - \frac{m^2}{\rho^2}\right)\psi_{m1} = 0 \quad (12)$$

which can be related to the known equation [Olver, 1964]

$$w'' + \left(\frac{1-2p}{z}\right)w' + \left(\lambda^2 q^2 z^{2q-2} + \frac{p^2 - v^2 q^2}{z^2}\right)w = 0 \quad (13)$$

having solutions of the form

$$w = z^p \mathcal{C}_v(\lambda z^q) \quad (14)$$

where  $\mathcal{C}_v()$  is any Bessel function. Comparing the coefficients of (12) and (13) we find that the solutions to (12) must have the form

$$\psi_{m1} : \rho^p \mathcal{C}_v(\lambda \rho^{p+1}) \quad (15a)$$

where

$$\lambda = \frac{k_0}{(p+1)b^p} \quad (15b)$$

$$v = \frac{\sqrt{m^2 + p^2}}{p+1} \quad (15c)$$

The solution (15a) is evidently valid for all  $p \neq -1$  and when  $p = 0$  it becomes identical to the corresponding solution in free space.

### 2.1 The Case $p \neq -1$

The complete solution can in this case be written in the following form

$$H_{z1} = \rho^p \sum_{-\infty}^{\infty} e^{im\phi} [C_m J_\nu(\lambda \rho^{p+1}) + D_m H_\nu^{(1)}(\lambda \rho^{p+1})] \quad (16a)$$

$$H_{z0} = \sum_{-\infty}^{\infty} e^{im\phi} F_m H_m^{(1)}(k_0 \rho) . \quad (16b)$$

Noting that the tangential electric field components are expressed as follows

$$E_{\phi 1} = \frac{-i}{\omega \epsilon_0} \left(\frac{b}{\rho}\right)^{2p} \frac{\partial H_{z1}}{\partial \rho} \quad (17a)$$

$$E_{\phi 0} = \frac{-i}{\omega \epsilon_0} \frac{\partial H_{z0}}{\partial \rho} \quad (17b)$$

one obtains, applying the boundary conditions at  $\rho = a$  and  $\rho = b$ , the set of simultaneous algebraic equations

$$\begin{pmatrix} a_{11} & a_{12} & 0 \\ a_{21} & a_{22} & a_{23} \\ a_{31} & a_{32} & a_{33} \end{pmatrix} \begin{pmatrix} C_m \\ D_m \\ F_m \end{pmatrix} = \frac{i\omega \epsilon_0 V}{2\pi a b^{2p}} \begin{pmatrix} 1 \\ 0 \\ 0 \end{pmatrix} \quad (18)$$

where

$$\begin{aligned} a_{11} &= \frac{k_0}{b^p} \left[ J_\nu'(A) + \frac{p}{B_0} \left(\frac{b}{a}\right)^{p+1} J_\nu(A) \right] \\ a_{12} &= \frac{k_0}{b^p} \left[ H_\nu^{(1)'}(A) + \frac{p}{B_0} \left(\frac{b}{a}\right)^{p+1} H_\nu^{(1)}(A) \right] \\ a_{21} &= b^p J_\nu(B) \\ a_{22} &= b^p H_\nu^{(1)}(B) \\ a_{23} &= -H_m^{(1)}(B_0) \\ a_{31} &= b^p \left[ J_\nu'(B) + \frac{p}{B_0} J_\nu(B) \right] \\ a_{32} &= b^p \left[ H_\nu^{(1)'}(B) + \frac{p}{B_0} H_\nu^{(1)}(B) \right] \\ a_{33} &= -H_m^{(1)'}(B_0) \end{aligned} \quad (19)$$

and

$$A_0 = k_0 a$$

$$B_0 = k_0 b$$

$$A = \frac{A_0}{p+1} \left(\frac{a}{b}\right)^p$$

$$B = \frac{B_0}{p+1} \quad . \quad (20)$$

The system of simultaneous equations can be solved readily using Cramer's rule. The field in the air is found to be

$$H_{z0} = \frac{-\omega \epsilon_0 (p+1) V}{\pi^2 A_0 B_0} \sum_{-\infty}^{\infty} e^{im\phi} \frac{H_m^{(1)}(k_0 \rho)}{\Delta_m} \quad (21)$$

where

$$\Delta_m = P_\nu H_m^{(1)}(B_0) - Q_\nu H_m^{(1)'}(B_0) \quad (22)$$

and

$$\begin{aligned} P_\nu = & \left[ J_\nu'(A) + \frac{p}{B_0} \left(\frac{b}{a}\right)^{p+1} J_\nu(A) \right] \left[ H_\nu^{(1)'}(B) + \frac{p}{B_0} H_\nu^{(1)}(B) \right] \\ & - \left[ H_\nu^{(1)'}(A) + \frac{p}{B_0} \left(\frac{b}{a}\right)^{p+1} H_\nu^{(1)}(A) \right] \left[ J_\nu'(B) + \frac{p}{B_0} J_\nu(B) \right] \quad (23a) \end{aligned}$$

$$\begin{aligned} Q_\nu = & H_\nu^{(1)}(B) \left[ J_\nu'(A) + \frac{p}{B_0} \left(\frac{b}{a}\right)^{p+1} J_\nu(A) \right] \\ & - J_\nu(B) \left[ H_\nu^{(1)'}(A) + \frac{p}{B_0} \left(\frac{b}{a}\right)^{p+1} H_\nu^{(1)}(A) \right] \quad . \end{aligned}$$

As a partial check on the above result, we set  $p = 0$  which corresponds to a cylinder in the air. In this case one finds

$$\Delta_m = \frac{2i}{\pi b} H_m^{(1)'}(A_0) \quad (24)$$

which upon substitution into (21) gives

$$H_{z0} = \frac{iV}{2\pi Z_0 a} \sum_{-\infty}^{\infty} e^{im\phi} \frac{H_m^{(1)}(k_0 \rho)}{H_m^{(1)'}(A_0)} \quad (25)$$

where  $Z_0 = (\mu_0/\epsilon_0)^{1/2}$  is the free space impedance. The expression in (25) can be recognized as the one appropriate to an axially slotted cylinder in free space [Wait, 1959].

Another partial check can be performed setting  $b = a$ . In this case one finds

$$\Delta_m = \frac{2i(p+1)}{\pi a} H_m^{(1)'}(A_0) \quad (26)$$

which when substituted into (21) again gives (25) as it should.

## 2.2 The Case $p = -1$

In the previous case we have excluded the case  $p = -1$  because the solution to the radial wave function was not defined therein. We shall now examine this particular case in detail.

Putting  $p = -1$  in (12) one obtains

$$\psi_{m1}'' + \frac{3}{\rho} \psi_{m1}' + \frac{B_0^2 - m^2}{\rho^2} \psi_{m1} = 0 \quad (27)$$

This differential equation has simple solutions

$$\psi_{m1} : \rho^{-1+q} \quad , \quad \rho^{-1-q}$$

$$q = \sqrt{1 + m^2 - B_0^2} \quad (28)$$



The field in the air now becomes

$$H_{z0} = \frac{i\omega\epsilon_0 bV}{\pi a} \sum_{-\infty}^{\infty} \frac{e^{im\phi} q(ab)^q H_m^{(1)}(k_0\rho)}{B_0 H_m^{(1)'}(B_0) [(q-1)a^{2q} + (q+1)b^{2q}] + (1-q^2) H_m^{(1)}(B_0) [b^{2q} - a^{2q}]}$$

(29)

As a partial check on this result one can set  $a = b$  in which case one again obtains (25).

Inasmuch as this solution is of rather restrictive application, it will not be pursued any further.

### 3. Application to Small Cylinders

The formulas (21) and (29) constitute the formal solution to the problem for any inhomogeneous layer described by (11) and any radius of the cylinder. In the case when the radii of the cylinder and the coating are small, considerable simplifications to these formulas are possible.

It will be convenient to rewrite (21) in the form

$$H_{z0} = \frac{-\omega\epsilon_0(p+1)V}{\pi^2 A_0 B_0} \sum_0^{\infty} \epsilon_m \cos m\phi \frac{H_m^{(1)}(k_0\rho)}{\Delta_m}$$

$$\epsilon_m = \begin{cases} 1 & , m = 0 \\ 2 & , m \neq 0 \end{cases} .$$

(30)

Now if the radius of the coating is sufficiently small so that

$$B_0 \ll p + 1$$

(31)

the following approximations to the various Bessel functions are possible

$$\begin{aligned}
 J_\nu(x) &\sim \frac{1}{\Gamma(\nu+1)} \left(\frac{x}{2}\right)^\nu; & J'_\nu(x) &\sim \frac{\nu}{x} J_\nu(x) \\
 H_\nu^{(1)}(x) &\sim \frac{-i \Gamma(\nu)}{\pi} \left(\frac{x}{2}\right)^\nu; & H_\nu^{(1)'}(x) &\sim \frac{-\nu}{x} H_\nu^{(1)}(x).
 \end{aligned} \tag{32}$$

Using these approximations in (21), one obtains its approximate form valid for  $B_0 \ll p + 1$ ,  $p \neq -1$ .

$$H_{z0} = \frac{\omega \epsilon_0 V}{4} \left[ H_0^{(1)}(k_0 \rho) - 8 \left(\frac{a}{b}\right)^p \sum_{l=1}^{\infty} \left(\frac{B_0}{2}\right)^m \frac{\sqrt{m^2+p^2} \cos m\phi}{m! R_m} H_m^{(1)}(k_0 \rho) \right] \tag{33}$$

where

$$R_m = (m-p-\sqrt{m^2+p^2}) \left(\frac{a}{b}\right)^{\sqrt{m^2+p^2}} - (m-p+\sqrt{m^2+p^2}) \left(\frac{a}{b}\right)^{-\sqrt{m^2+p^2}}. \tag{34}$$

It will be noted that the first term in (33) correctly represents the field of an isolated magnetic current line source of the strength  $I^{(m)} = -V$ . The remainder of the terms in (33) evidently represents the correction terms for the non-zero radius of the cylinder and the effect of the coating.

#### 4. Application to Large Cylinders

When the radii of the cylinder and the coating are not small, the harmonic series representative of the solution derived earlier is slowly convergent and consequently many terms are needed for a given degree of accuracy. In this case, an alternate, integral representation of the solution can be found using the well-known Watson Transformation. Subsequently, this integral representation can be used to find the "residue series representation" valid in the shadow region and the "geometric optics field" valid in the illuminated region.

#### 4.1 Integral Representation of the Solution

If the denominator  $\Delta_\mu$  in (21) has no zeroes on the real axis in the complex  $\mu$ -plane, then it will follow that the harmonic series representation (21) can be put in the form

$$H_{z0} = \frac{\omega \epsilon_0 (p+1) V}{i 2 \pi^2 A_0 B_0} \int_C \frac{H_\mu^{(1)}(k_0 \rho)}{\Delta_\mu} \cdot \frac{e^{i\mu(\phi-\pi)}}{\sin \mu \pi} d\mu \quad (35)$$

where  $C$  is a contour in the complex  $\mu$  - plane that runs slightly above and slightly below the real axis in the clockwise direction in such a way that it encloses all of the zeroes of  $\sin \mu \pi$ . Alternately (35) can be written in the form

$$H_{z0} = \frac{\omega \epsilon_0 (p+1) V}{i \pi^2 A_0 B_0} \int_{-\infty}^{\infty} \frac{H_\mu^{(1)}(k_0 \rho)}{\Delta_\mu} \cdot \frac{\cos \mu(\phi-\pi)}{\sin \mu \pi} d\mu \quad (36)$$

where the path of integration is understood to run slightly above the real axis.

#### 4.2 Fields in the Shadow Region

In order to find the residue series representation we must evaluate the integral in (36) by closing the contour with a large semi-circle in the upper half plane enclosing all of the poles produced by the zeroes of  $\Delta_\mu$ . To this end we must investigate the behavior of the integrand in (36) for large values of  $\mu$ .

Let us divide the upper half-plane as follows:

- Region I:  $0 < \arg \mu < \pi/2 - \delta$
- Region II:  $\pi/2 - \delta < \arg \mu < \pi/2 + \delta$
- Region III:  $\pi/2 + \delta < \arg \mu < \pi$

and note the following asymptotic behavior of the Bessel functions [Hönl et al, 1961]

$$\text{I: } H_{\mu}^{(1)}(x) \sim i \sqrt{\frac{2}{\pi\mu}} \left(\frac{2\mu}{ex}\right)^{\mu}, \quad J_{\mu}(x) \sim \frac{1}{\sqrt{2\pi\mu}} \left(\frac{2\mu}{ex}\right)^{-\mu} \quad (37a)$$

$$\text{II: } H_{\mu}^{(1)}(x) \sim \sqrt{\frac{2}{\pi\mu}} \left(\frac{2\mu}{ex}\right)^{-\mu}, \quad J_{\mu}(x) \sim \frac{i}{\sqrt{2\pi\mu}} \left(\frac{2\mu}{ex}\right)^{\mu} \quad (37b)$$

$$\text{III: } H_{\mu}^{(1)}(x) \sim -i \sqrt{\frac{2}{-\pi\mu}} e^{-i\mu\pi} \left(\frac{-2\mu}{ex}\right)^{\mu}, \quad J_{\mu}(x) \sim \frac{-\sin\mu\pi}{\sqrt{-2\pi\mu}} \left(\frac{-2\mu}{ex}\right)^{-\mu}. \quad (37c)$$

Using these asymptotic forms, (22) can be written

$$(\Delta_{\mu})_{\text{I}} \sim \frac{i2\mu}{\pi AB_0} \left(\frac{b}{a}\right)^{\mu} H_{\mu}^{(1)}(B_0) \quad (38a)$$

$$(\Delta_{\mu})_{\text{II}} \sim \frac{i2\mu}{\pi AB_0} \left(\frac{b}{a}\right)^{-\mu} H_{\mu}^{(1)}(B_0) \quad (38b)$$

$$(\Delta_{\mu})_{\text{III}} = \frac{ivp^2}{2AB_0\mu} X_{\nu} H_{\mu}^{(1)}(B_0) \quad (38c)$$

where

$$X_{\nu} = J_{\nu}(A)Y_{\nu}(B) - J_{\nu}(B)Y_{\nu}(A). \quad (39)$$

The asymptotic evaluation of  $X_{\nu}$  in (39) is somewhat cumbersome inasmuch as the straightforward application of (37c) yields a value of zero. In order to obtain a more accurate estimate, one may apply the multiplication theorem for the Bessel functions [Olver, 1962]

$$\zeta_{\nu}(A) = \zeta_{\nu}(aB) = \alpha^{\nu} \sum_{n=0}^{\infty} \frac{(1-\alpha)^n}{n!} \left(\frac{B}{2}\right)^n \zeta_{\nu+n}(B) \quad (40a)$$

with

$$\alpha = \left(\frac{a}{b}\right)^{p+1} . \quad (40b)$$

Substituting (40a) into (39) gives

$$X_\nu = \alpha^\nu \sum_{n=0}^{\infty} \frac{(1-\alpha^2)^n}{n!} \left(\frac{B}{2}\right)^n \left[ Y_\nu(B) J_{\nu+n}(B) - J_\nu(B) Y_{\nu+n}(B) \right] . \quad (41)$$

Now using the Wronskian

$$Y_\nu(B) J_{\nu+1}(B) - Y_{\nu+1}(B) J_\nu(B) = \frac{2}{\pi B} \quad (42)$$

and the recurrence relation

$$\zeta_{\nu+2}(B) = \frac{2(\nu+1)}{B} \zeta_{\nu+1}(B) - \zeta_\nu(B) \quad (43)$$

which for a large  $\nu$  can be approximated by

$$\zeta_{\nu+n}(B) \sim \left(\frac{2\nu}{B}\right)^{n-1} \zeta_{\nu+1}(B) - \left(\frac{2\nu}{B}\right)^{n-2} \zeta_\nu(B), \quad (44)$$

one can sum the series in (41) to obtain

$$X_\nu \sim \frac{\alpha^\nu}{\pi\nu} (e^{\nu(1-\alpha^2)} - 1) . \quad (45)$$

In region III,  $\mu$  and consequently  $\nu$  will have a negative real part so that the exponential in (45) will have negligible contribution. Thus (38c) becomes

$$(\Delta_\mu)_{\text{III}} \sim \frac{ip^2}{2\pi AB_0\mu} \left(\frac{a}{b}\right)^\mu H_\mu^{(1)}(B_0) . \quad (46)$$

Setting  $\mu = R \exp(i\theta)$  on the semicircle, it is now easy to show that for a large  $R$

$$\begin{aligned} \left| \frac{H_{\mu}^{(1)}(k_0 \rho) \cos \mu(\phi - \pi) d\mu}{\Delta_{\mu} \sin \mu \pi} \right| &\sim e^{-R[\gamma \sin \theta + \cos \theta \ln(\rho/a)]} \\ &\sim e^{-R[\gamma \sin \theta - \cos \theta \ln(\rho/a)]} \\ &\sim R^2 e^{-R[\gamma \sin \theta - \cos \theta \ln(\rho/a)]} \end{aligned} \quad (47)$$

in regions I, II, and III respectively, where  $\gamma = \phi$  for  $0 < \phi < \pi$  and  $\gamma = 2\pi - \phi$  for  $\pi < \phi < 2\pi$ . Thus the contribution from the large semicircular arc vanishes everywhere in the upper half plane.

The integral in (36) can now be evaluated to give

$$H_{z0} = \frac{2\omega \epsilon_0 (p+1) V}{\pi A_0 B_0} \sum_{n=1}^{\infty} C_n H_{\mu_n}^{(1)}(k_0 \rho) \frac{\cos \mu_n(\phi - \pi)}{\sin \mu_n \pi} \quad (48a)$$

where

$$C_n = \left( \frac{\partial}{\partial \mu} \Delta_{\mu} \Big|_{\mu=\mu_n} \right)^{-1} \quad (48b)$$

and  $\mu_n$  are the zeroes of  $\Delta_{\mu} = 0$ .

In the far zone, the Hankel function can be replaced by its asymptotic form

$$H_{\mu_n}^{(1)}(k_0 \rho) \sim \sqrt{\frac{2}{\pi k_0 \rho}} e^{i(k_0 \rho - \pi/4 - \mu_n \pi/2)} \quad (49)$$

and noting that

$$\frac{\cos \mu_n(\phi - \pi)}{\sin \mu_n \pi} e^{-i\mu_n \pi/2} \sim -i \left[ e^{i\mu_n(3\pi/2 - \phi)} + e^{i\mu_n(\phi - \pi/2)} \right] \quad (50)$$

it will follow that the series, in (48) will converge rapidly in the shadow region of the slot,  $\pi/2 < \phi < 3\pi/2$ .

The zeroes of  $\Delta_{\mu n} = 0$  are evaluated approximately in the Appendix.

### 4.3 Fields in the Illuminated Region

To find the fields in the region directly illuminated by the slot we must evaluate the integral in (36) at its stationary points. In what follows it will be shown that these stationary points will be found on the real axis. In order to assure freedom in deforming the contour of integration so as not to interfere with the poles of the integrand due to the zeroes of  $\sin \mu \pi$ , it will be convenient to employ the transformation

$$\frac{\cos \mu(\phi - \pi)}{\sin \mu \pi} = \frac{\cos \mu \phi}{\sin \mu \pi} e^{i\mu\pi} - ie^{i\mu\phi} \quad (51)$$

which enables writing (36) in the form

$$H_{z0} = \frac{-\omega \epsilon_0 (p+1)V}{\pi^2 A_0 B_0} (iI_1 + I_2) \quad (52)$$

where

$$I_1 = \int_{-\infty}^{\infty} \frac{H_{\mu}^{(1)}(k_0 \rho)}{\Delta_{\mu}} \cdot \frac{\cos \mu \phi}{\sin \mu \pi} e^{i\mu\pi} d\mu \quad (53)$$

and

$$I_2 = \int_{-\infty}^{\infty} \frac{H_{\mu}^{(1)}(k_0 \rho)}{\Delta_{\mu}} e^{i\mu\phi} d\mu. \quad (54)$$

The integral  $I_1$  can be readily evaluated by closing the contour with a large semicircle in the upper half-plane, the contribution of which is negligible, and integrating about the poles produced by the zeroes of

$\Delta_{\mu_n} = 0$ . The result is

$$I_1 = 2\pi i \sum_{n=1}^{\infty} C_n H_{\mu_n}^{(1)}(k_0 \rho) \frac{\cos \mu_n \phi}{\sin \mu_n \pi} e^{i\mu_n \pi} \quad (55)$$

Using the asymptotic form of the Hankel function in (49) and a simple transformation, one can readily show that in the far zone

$$I_1 = 2 \sqrt{\frac{2\pi}{k_0 \rho}} e^{i(k_0 \rho - \pi/4)} \sum_{n=1}^{\infty} C_n \left[ \frac{e^{i\mu_n(3\pi/2+\phi)} + e^{i\mu_n(3\pi/2-\phi)}}{1 - e^{i2\pi\mu_n}} \right] \quad (56)$$

Since  $\mu_n$  has a positive imaginary part it will follow that the contribution of  $I_1$  in the illuminated region will be small.

To evaluate the integral  $I_2$  we first note the following asymptotic forms valid for a large value of the argument [Hönl et al, 1961]

$$H_{\mu}^{(1)}(B_0) \sim \sqrt{\frac{2}{\pi}} (B_0^2 - \mu^2)^{-1/4} e^{i[\sqrt{B_0^2 - \mu^2} - \mu \arccos \frac{\mu}{B_0} - \pi/4]}, \quad |\mu| < B_0 \quad (57a)$$

and

$$H_{\mu}^{(1)}(B_0) \sim -i \sqrt{\frac{2}{\pi}} (\mu^2 - B_0^2)^{-1/4} e^{\mu \ln \left( \frac{\mu + \sqrt{\mu^2 - B_0^2}}{B_0} \right) - \sqrt{\mu^2 - B_0^2}}, \quad |\mu| > B_0 \quad (57b)$$

If we denote by  $I_{2\leq}$  the value of integral in (54) evaluated for  $|\mu| < B_0$  and  $I_{2>}$  for  $|\mu| > B_0$  respectively, then we can write

$$I_2 = B_0 \int \frac{(B_0^2 - \mu^2)^{1/4} e^{if < d_{\mu}}}{[(k_0 \rho)^2 - \mu^2]^{1/4} [B_0 P_V - i(B_0^2 - \mu^2)^{1/2} Q_V]} \quad (58a)$$



and

$$I_{2>} = B_0 e^{i\pi/4} \int \frac{(\mu^2 - B_0^2)^{1/4} e^{if_{>}} d\mu}{[(k_0\rho)^2 - \mu^2]^{1/4} [B_0 P_V + (\mu^2 - B_0^2)^{1/2} Q_V]} \quad (58b)$$

where

$$f_{<} = \mu\phi + \sqrt{(k_0\rho)^2 - \mu^2} - \sqrt{B_0^2 - \mu^2} - \mu(\arccos \frac{\mu}{k_0\rho} - \arccos \frac{\mu}{B_0}) \quad (59a)$$

and

$$f_{>} = i(\mu\phi + \sqrt{(k_0\rho)^2 - \mu^2} - \mu \arccos \frac{\mu}{k_0\rho}) - \mu \ln \left( \frac{\mu + \sqrt{\mu^2 - B_0^2}}{B_0} \right) + \sqrt{\mu^2 - B_0^2} \quad (59b)$$

Setting  $f_{<}^1 = 0$  determines the stationary points of the integrals.

It will follow that the stationary points will be given by

$$\mu_s = \pm B_0 \sin \phi \quad (60)$$

which are within the limits of  $I_{2<}$  but not of  $I_{2>}$ . Hence, using the method of stationary phase, the integral  $I_2$  is evaluated to give

$$I_2 \sim \sqrt{\frac{2\pi}{k_0\rho}} \frac{B_0 \cos \phi e^{i(k_0\rho - B_0 \cos \phi - \pi/4)}}{P_V(\mu_s) - i \cos \phi Q_V(\mu_s)} \quad (61)$$

with

$$v = \frac{\sqrt{B_0^2 \sin^2 \phi + p^2}}{1 + p} \quad (62)$$

Comparing (56) and (61) it will be noticed that the contribution of the former is negligible in relation to the latter, hence (52) becomes

$$H_{z0} = \frac{-(p+1)V}{\pi a z_0} \sqrt{\frac{2}{\pi k_0 \rho}} \cdot \frac{\cos \phi e^{i(k_0 \rho - B_0 \cos \phi - \pi/4)}}{P_V(\mu_S) - i \cos \phi Q_V(\mu_S)} \quad (63)$$

Two partial checks,  $b = a$  and  $p = 0$ , can be performed on (63) to obtain the well-known result for a bare cylinder. In the first case,  $b = a$ , one readily obtains

$$P_V(\mu_S) = 0$$

$$Q_V(\mu_S) = \frac{-2i(p+1)}{\pi A_0} \quad (64)$$

which together with (63) gives the well-known result [Wait, 1959]

$$H_{z0} = \frac{V}{z_0} \sqrt{\frac{k_0}{2\pi\rho}} e^{i(k_0 \rho - A_0 \cos \phi - \pi/4)} \quad (65)$$

For the case  $p = 0$ , noting that  $H_{\mu_S}^{(1)'}(B_0)/H_{\mu_S}^{(1)}(B_0) = i \cos \phi$ , one obtains

$$\begin{aligned} P_V(\mu_S) - i \cos \phi Q_V(\mu_S) &= \frac{2i}{\pi B_0} \cdot \frac{H_{\mu_S}^{(1)'}(A_0)}{H_{\mu_S}^{(1)}(B_0)} \\ &\sim \frac{-2 \cos \phi}{\pi A_0} \quad (66) \end{aligned}$$

where the last approximation is valid if both  $A_0$  and  $B_0$  are large and not far apart. Substitution of (66) into (63) again yields (65) as it should.

## 5. Numerical Results and Interpretation

The power radiation patterns related to the field formula (63) are shown in Figs. 3 to 5. It will be noted that each pattern exhibits peaks at certain angles that appear to be a function of the cylinder radius,  $A_0$ ,

inhomogeneity gradient,  $p$ , and the thickness of the layer in wavelength  $\tau$ . These patterns resemble in many respects the radiation patterns of the corresponding planar geometry, homogeneous layer problem considered previously by several authors [Tamir and Oliner, 1962; Omura, 1962; Tyras et al, 1964] and the curved homogeneous layer considered by [Hasserjian, 1965].

The presence of the peaks in the radiation patterns as well as their relative position which is dependent on the geometry of the problem, can be explained qualitatively by the elementary consideration of geometric optics. Since all of the rays radiated by the source must satisfy the Snell's law

$$\sqrt{\epsilon(\rho)} \sin \phi(\rho) = \text{Const.} \quad (67)$$

any ray launched at an angle  $\phi(a)$  by the slot will be deflected while traveling through the layer according to

$$\phi(\rho) = \text{arc sin} \left[ \left( \frac{a}{\rho} \right)^p \sin \phi(a) \right] \quad (68)$$

Consequently, the angle that any ray will emerge from the layer,  $\phi(b)$ , will be given by

$$\phi(b) = \text{arc sin} \left[ \left( \frac{a}{b} \right)^p \sin \phi(a) \right] \quad (69)$$

It will follow that the angle  $\phi(b)$  increases with increasing radius of the cylinder,  $a$ , and it decreases with increasing outer radius of the layer,  $b$ , and an increasing gradient of the inhomogeneity as measured by the parameter 'p'. Moreover, since all of the rays launched by the slot are deflected in the layer toward the vertical axis according to (68), it will follow that there will be little, if any, broadside radiation by this structure. The pictorial representation of the foregoing, qualitative, analysis is shown in Fig. 6.

The examination of the various power radiation patterns shown in Figs. 3 to 5 reveals good agreement with the qualitative arguments of geometric optics. In particular, the presence of the minor side lobes in Fig. 5 must be attributed to the phase interference effects of some emerging rays that occur under a certain set of conditions.

## 6. Figures

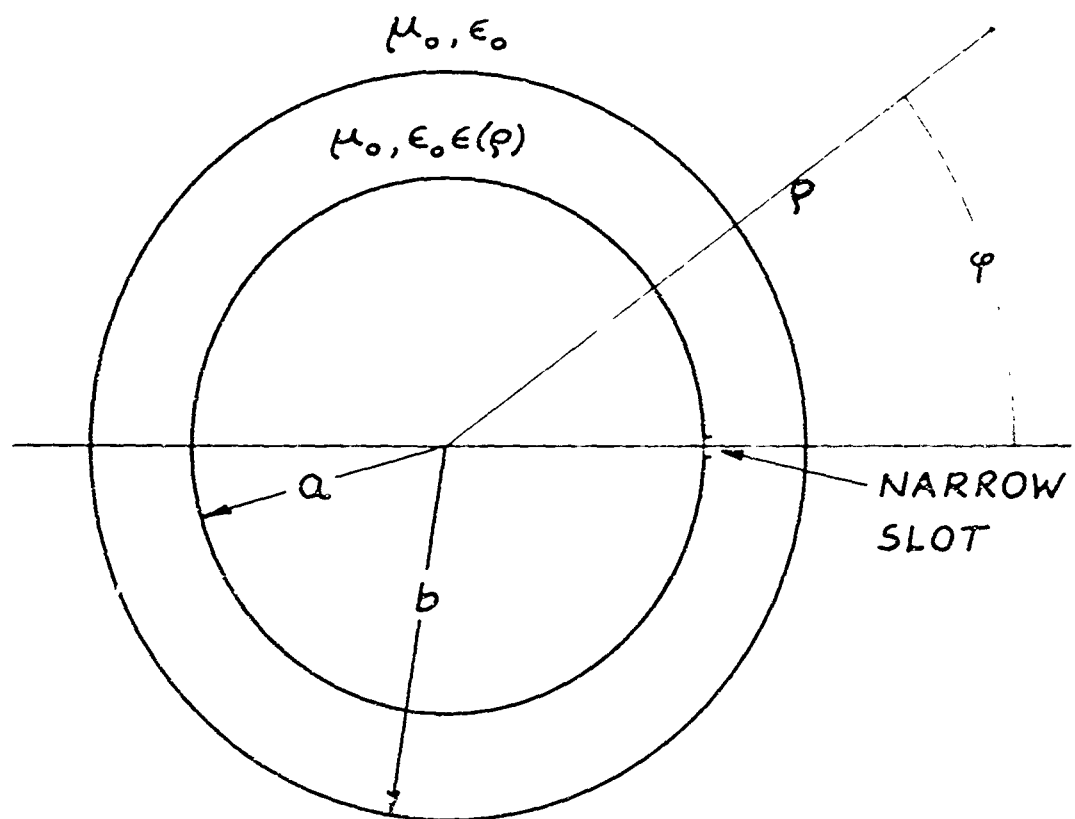


Fig. 1. Geometry of the problem

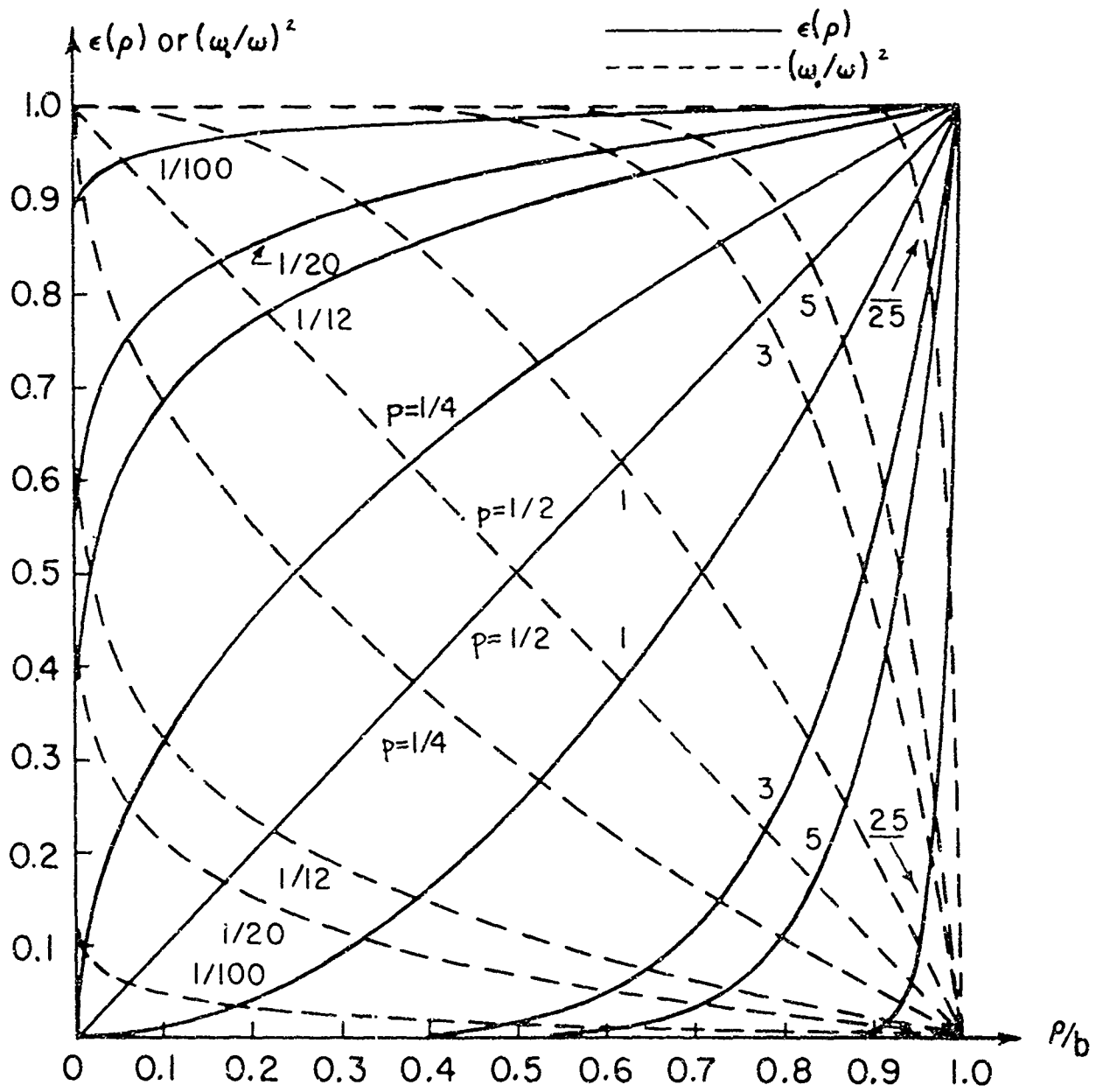


Fig. 2a. Inhomogeneous sheath profile (increasing)

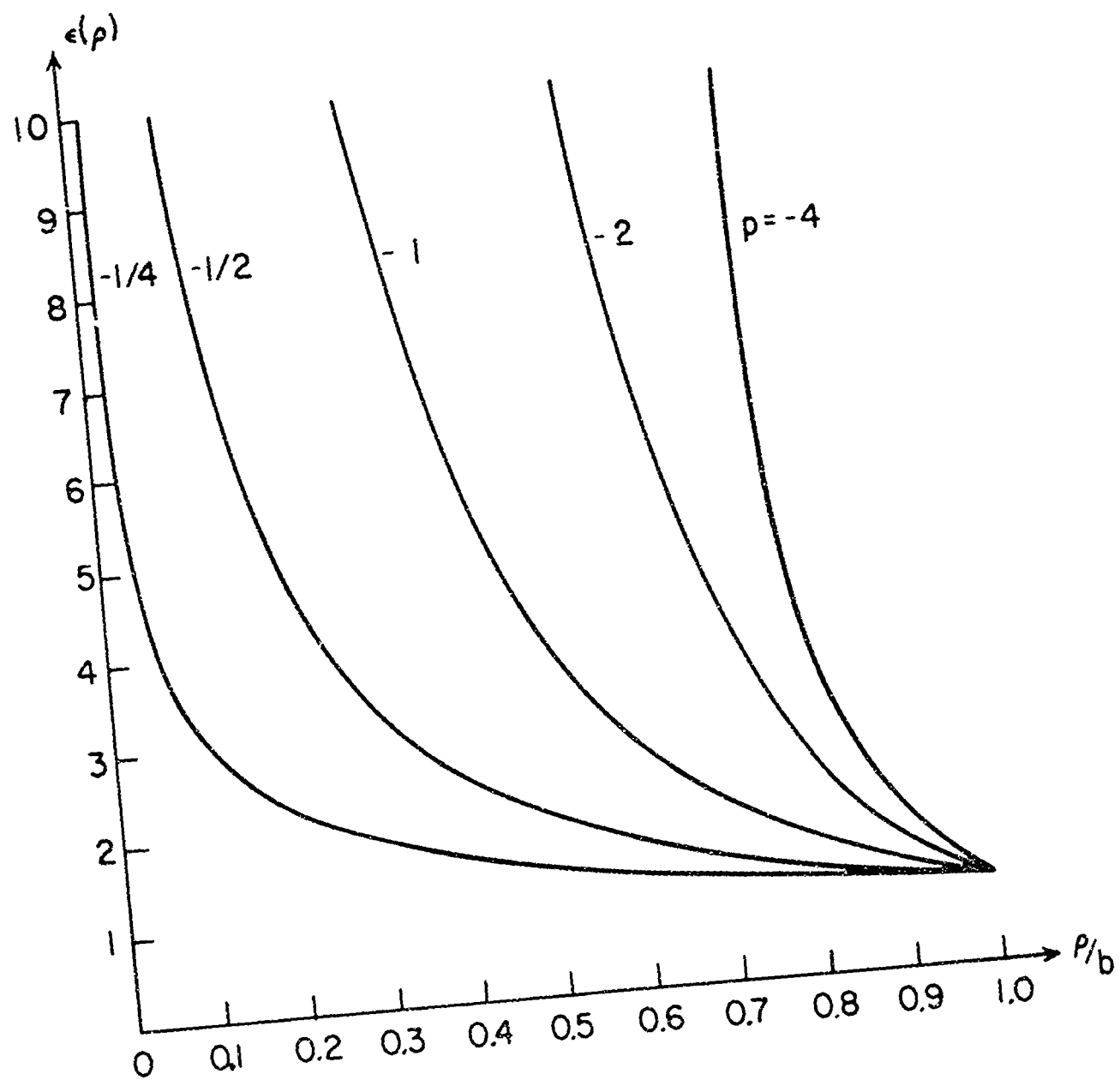


Fig. 2b. Inhomogeneous sheath profile (decreasing)

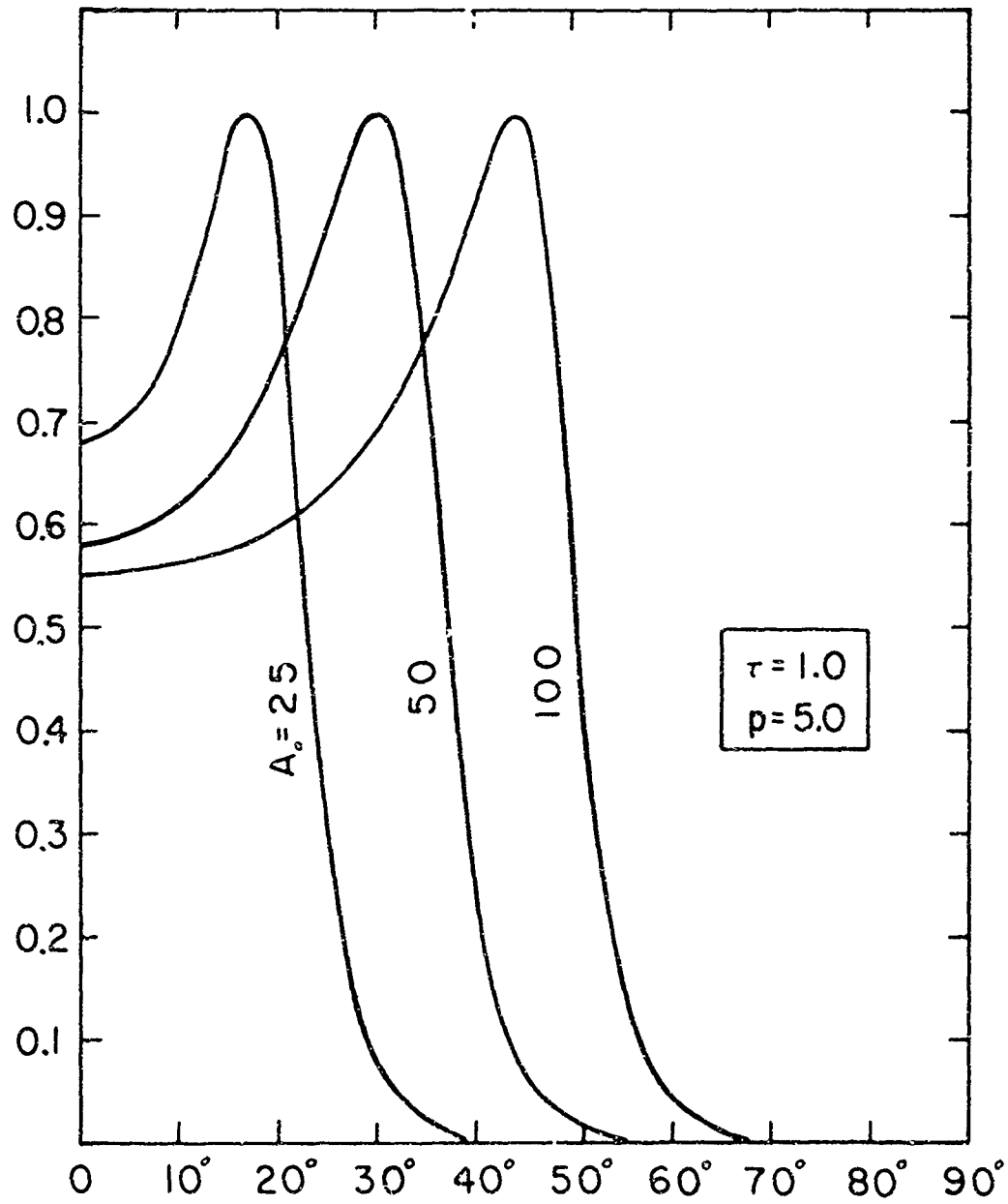


Fig. 3. Variation of the radiation pattern as a function of the cylinder radius

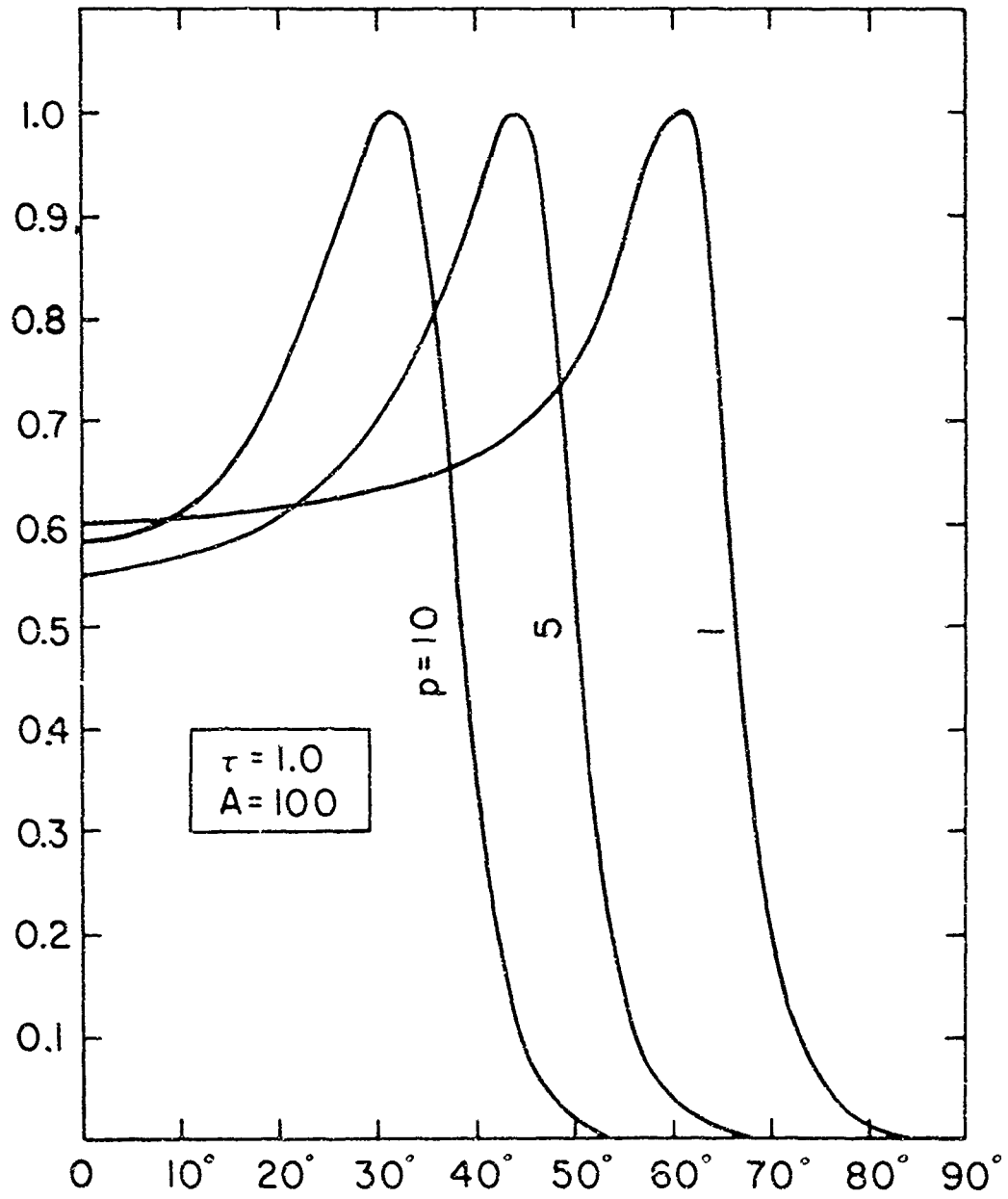


Fig. 4. Variation of the radiation pattern as a function of the inhomogeneity gradient



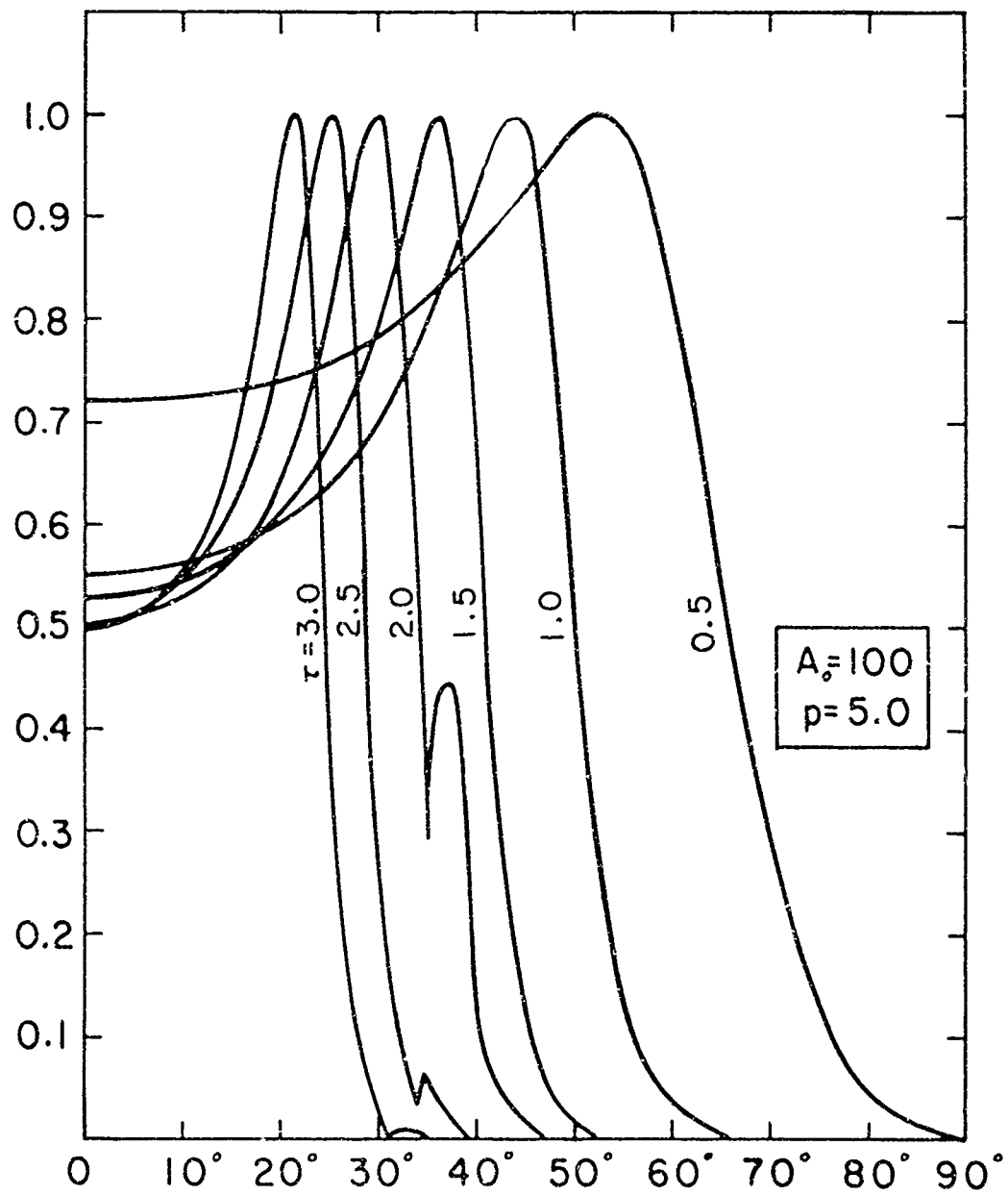


Fig. 5. Variation of the radiation pattern as a function of the layer thickness

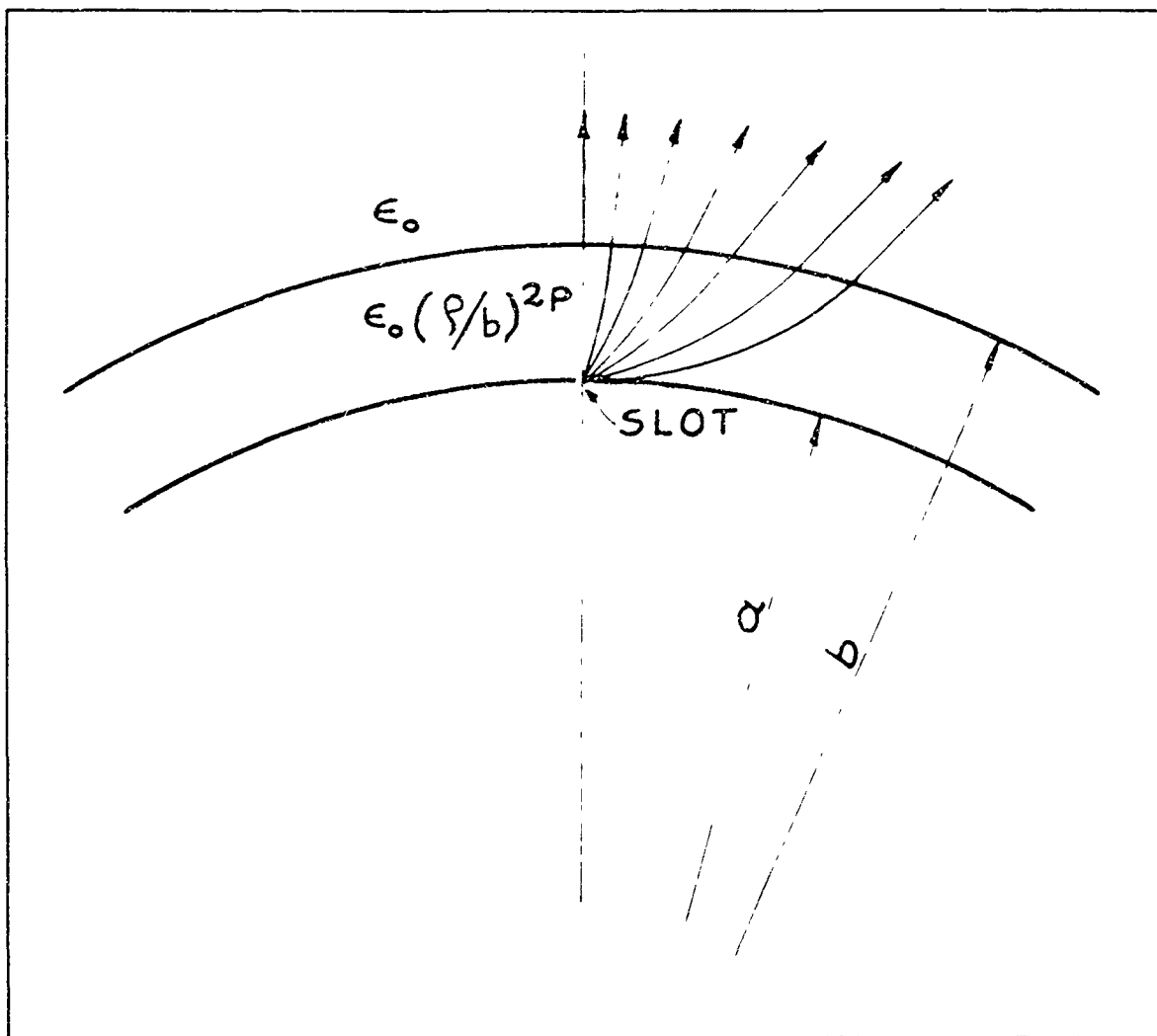


Fig. 6. Ray focusing by the layer

## 7. Appendix

The Roots of  $\Delta_{\mu_n} = 0$ 

From (22) we have in this case

$$\frac{H_{\mu_n}^{(1)'}(B_0)}{H_{\mu_n}^{(1)}(B_0)} = \frac{P_V}{Q_V} \quad (\text{A-1})$$

we note

$$\begin{aligned} B - A &= tB \\ t &= 1 - \left(\frac{a}{b}\right)^{p+1} \end{aligned} \quad (\text{A-2})$$

When the radii of the cylinder and the coating are large and not far apart, then the quantity 't' in (A-2) will necessarily be small. In this case we can use the approximation

$$\zeta_V(A) \sim \zeta_V(B) - tB \zeta_V'(B) \quad (\text{A-3})$$

where  $\zeta_V(\ )$  is any Bessel function. Using (A-3) in (A-1) one obtains the following approximate expression

$$\frac{H_{\mu_n}^{(1)'}(B_0)}{H_{\mu_n}^{(1)}(B_0)} = \frac{1}{(p+1)B_0} \left[ 1 - \left(\frac{a}{b}\right)^{p+1} \right] (\mu_n^2 - B_0^2) \quad (\text{A-4})$$

Note that when  $a = b$  then the right side of (A-4) is zero and the expression reduces  $H_{\mu_n}^{(1)'}(B_0) = 0$  which is appropriate to a bare cylinder.

It is easy to show using asymptotic form for the Hankel functions that (A-4) will have no solutions if  $\mu < B_0$ .

In the range  $\mu \sim B_0$ , where  $B_0$  is large, one can use the transition region expansion of the Hankel functions in terms of Airy functions [Hönl et al, 1961] to obtain

$$\frac{H_{\mu_n}^{(1)'}(B_0)}{H_{\mu_n}^{(1)}(B_0)} = - \left(\frac{2}{B_0}\right)^{1/3} e^{i2\pi/3} \frac{\text{Ai}'\left[\left(\frac{2}{B_0}\right)^{1/3} e^{-i\pi/3}(B_0 - \mu_n)\right]}{\text{Ai}\left[\left(\frac{2}{B_0}\right)^{1/3} e^{-i\pi/3}(B_0 - \mu_n)\right]} \quad (\text{A-5})$$

Substituting (A-5) into (A-4) we write

$$\frac{(B_0^2 - \mu_n^2) e^{-i2\pi/3}}{(p+1) B_0^{2/3} 2^{1/3}} \left[1 - \left(\frac{a}{b}\right)^{p+1}\right] = \frac{\text{Ai}'\left[\left(\frac{2}{B_0}\right)^{1/3} e^{-i\pi/3}(B_0 - \mu)\right]}{\text{Ai}\left[\left(\frac{2}{B_0}\right)^{1/3} e^{-i\pi/3}(B_0 - \mu)\right]} \quad (\text{A-6})$$

The left side of (A-6) is small if 'a' and 'b' are large and not too far apart. Thus to the first approximation the roots will be determined from  $\text{Ai}'(a_n^i) = 0$  and consequently

$$\mu_n \sim B_0 - a_n^i \left(\frac{B_0}{2}\right)^{1/3} e^{i\pi/3} \quad (\text{A-7})$$

which are the roots appropriate to the bare cylinder.

Since the first root,  $\mu_1$ , is close to  $B_0$ , a better approximation to its value can be obtained by expanding the Airy function and its derivative in a power series. We note

$$\frac{\text{Ai}'(z)}{\text{Ai}(z)} = - \frac{C_2}{C_1} \left(1 + \frac{C_2}{C_1} z - \frac{C_1}{2C_2} z^2 + \dots\right) \quad (\text{A-8})$$

where  $C_2/C_1 \sim 0.72$  [Olver, 1962]. Setting  $B_0^2 - \mu_1^2 \sim 2B_0(B_0 - \mu_1)$  and collecting the above results, we obtain a better approximation for the first root as follows

$$\mu_1 \sim B_0 + \frac{\left(\frac{2}{B_0}\right)^{1/3} \frac{C_2}{C_1} (p+1) e^{i2\pi/3}}{\left(\frac{C_2}{C_1}\right)^2 \left(\frac{2}{B_0}\right)^{2/3} \cdot (p+1) e^{i\pi/3} + 2 \left[1 - \left(\frac{a}{b}\right)^{p+1}\right]} \quad (\text{A-9})$$

## REFERENCES

- Dettman, J. W. (1962), *Mathematical methods in physics and engineering*, (McGraw-Hill, Inc., New York).
- Hamm, J. M., and G. Tyras (July 1965), Further experimental study of plasma sheath effects on antennas, Engineering Experiment Station, U. of Ariz., Rep. No. 2, AFCRL-65-608, Contract AF 19(628)-3834.
- Harris, J. H., Radiation pattern characteristics of line sources in the presence of dielectric layers, Hughes Aircraft Co., Rep. No. P65-91, AFCRL-65-666 Contract 19(628)-4349.
- Harris, J. H., and J. Pachares (June 1965), The computation of cylindrical radiation problems, Hughes Aircraft Co., Rep. No. P65-79, AFCRL-65-610, Contract AF 19(62B)-4349.
- Hasserjian, G. (May, 1965), Fields of a curved plasma layer excited by a slot, *IEEE Trans. Antennas and Propagation*, AP-13, 389-395.
- Hönl, H., A. W. Maue and K. Westpfahl (1961), *Theorie der Beugung*, Handbuch der Physik, vol. XXV/1, edited by S. Flugge, Springer-Verlag, p. 504.
- Liu, Chao Han and L. Wetzel (June, 1965), Reflection electromagnetic waves from inhomogeneous plasma, Brown Univ. Sc. Rep. No. 6, AFCRL-65-334, Contr. No. 19(628)-2496.
- Olver, F. W. J. (June 1962), Bessel functions of integral order, *Handbook of Mathematical Functions*, edited by M. Abramowitz and I. A. Stegun, NBS App. Math. Series, 55.
- Omura, M. (December, 1962), Radiation pattern of a slit in a ground plane covered by a plasma layer, AFCRL-62-958.
- Rusch, W. V. T. (Jan. 1964), Radiation from an axially slotted cylinder with a radially inhomogeneous plasma coating, *Can. J. Phys.* 42, 26-42.
- Tamir, T., and A. A. Oliner, (January, 1962) The influence of complex waves on the radiation field of a slot-excited plasma layer, *IRE Trans. Antennas and Propagation* AP-10 55-65.
- Tyras, G., P. C. Bargelotes, J. M. Hamm and R. R. Schell, (June 1965), An experimental study of plasma sheath effects on antennas, *Radio Science Jour. Res. NBS/USNC-URSI*, 69D, 839-850.
- Wait, J. R. (1959), *Electromagnetic radiation from cylindrical structures*, (Pergamon Press).

Unclassified

Security Classification

DOCUMENT CONTROL DATA - R&D

(Security classification of title, body of abstract and indexing annotation must be entered when the overall report is classified)

1 ORIGINATING ACTIVITY (Corporate author) Engineering Experiment Station The University of Arizona Tucson, Arizona		2a REPORT SECURITY CLASSIFICATION Unclassified	
		2b GROUP	
3 REPORT TITLE Field of an Axially Slotted Circular Cylinder Clad with an Inhomogeneous Dielectric			
4 DESCRIPTIVE NOTES (Type of report and inclusive dates) Scientific Report (Interim) August, 1965 - January, 1966			
5 AUTHOR(S) (Last name, first name, initial) Tyras, George			
6 REPORT DATE February 1966		7a TOTAL NO OF PAGES 38	7b NO OF REFS 13
8a CONTRACT OR GRANT NO AF 19(628)-3834		9a ORIGINATOR'S REPORT NUMBER(S) No. 3	
b PROJECT NO and Task No. 4642,02			
c DOD element 62405 304		9b OTHER REPORT NO(S) (Any other numbers that may be assigned this report) AFCRL-66-203	
d DOD subelement 674642			
10 AVAILABILITY/LIMITATION NOTICES Distribution of this document is unlimited.			
11 SUPPLEMENTARY NOTES		12 SPONSORING MILITARY ACTIVITY Hq. AFCRL, OAR (CRD) United States Air Force L. G. Hanscom Field, Bedford, Mass.	
13 ABSTRACT Field expressions appropriate to small and large cylinders are found when the cylinder is coated with a layer of inhomogeneous dielectric of the form $\epsilon(\rho) = (\rho/b)^2 p$ , $a \leq \rho \leq b$ , where 'a' is the radius of the conducting cylinder, 'b' is the outer radius of the dielectric coating and 'p' is an arbitrary parameter. (U)  In the case of large cylinders coated with plasma, the radiation patterns are plotted for various combinations of the cylinder radius, thickness of the coating and the inhomogeneity gradient. The radiation patterns are in good agreement with qualitative arguments of geometric optics.(U)			

14 KEY WORDS	LINK A		LINK B		LINK C	
	ROLE	WT	ROLE	WT	ROLE	WT
Slot Antenna Plasma Sheath Radiation Pattern Inhomogeneous Dielectric Inhomogeneous Plasma						

INSTRUCTIONS

1. **ORIGINATING ACTIVITY** Enter the name and address of the contractor, subcontractor, grantee, Department of Defense activity or other organization (*corporate author*) issuing the report.

2a. **REPORT SECURITY CLASSIFICATION:** Enter the overall security classification of the report. Indicate whether "Restricted Data" is included. Marking is to be in accordance with appropriate security regulations.

2b. **GROUP:** Automatic downgrading is specified in DoD Directive S200.10 and Armed Forces Industrial Manual. Enter the group number. Also, when applicable, show that optional markings have been used for Group 3 and Group 4 as authorized.

3. **REPORT TITLE:** Enter the complete report title in all capital letters. Titles in all cases should be unclassified. If a meaningful title cannot be selected without classification, show title classification in all capitals in parenthesis immediately following the title.

4. **DESCRIPTIVE NOTES.** If appropriate, enter the type of report, e.g., interim, progress, summary, annual, or final. Give the inclusive dates when a specific reporting period is covered.

5. **AUTHOR(S).** Enter the name(s) of author(s) as shown on or in the report. Enter last name, first name, middle initial. If military, show rank and branch of service. The name of the principal author is an absolute minimum requirement.

6. **REPORT DATE.** Enter the date of the report as day, month, year, or month, year. If more than one date appears on the report, use date of publication.

7a. **TOTAL NUMBER OF PAGES** The total page count should follow normal pagination procedures, i.e., enter the number of pages containing information.

7b. **NUMBER OF REFERENCES.** Enter the total number of references cited in the report.

8a. **CONTRACT OR GRANT NUMBER** If appropriate, enter the applicable number of the contract or grant under which the report was written.

8b, 8c, & 8d. **PROJECT NUMBER** Enter the appropriate military department identification, such as project number, subproject number, system numbers, task number, etc.

9a. **ORIGINATOR'S REPORT NUMBER(S)** Enter the official report number by which the document will be identified and controlled by the originating activity. This number must be unique to this report.

9b. **OTHER REPORT NUMBER(S)** If the report has been assigned any other report numbers (*either by the originator or by the sponsor*), also enter this number(s).

10. **AVAILABILITY/LIMITATION NOTICES:** Enter any limitations on further dissemination of the report, other than those

imposed by security classification, using standard statements such as:

- (1) "Qualified requesters may obtain copies of this report from DDC."
- (2) "Foreign announcement and dissemination of this report by DDC is not authorized."
- (3) "U. S. Government agencies may obtain copies of this report directly from DDC. Other qualified DDC users shall request through \_\_\_\_\_."
- (4) "U. S. military agencies may obtain copies of this report directly from DDC. Other qualified users shall request through \_\_\_\_\_."
- (5) "All distribution of this report is controlled. Qualified DDC users shall request through \_\_\_\_\_."

If the report has been furnished to the Office of Technical Services, Department of Commerce, for sale to the public, indicate this fact and enter the price, if known.

11. **SUPPLEMENTARY NOTES** Use for additional explanatory notes.

12. **SPONSORING MILITARY ACTIVITY.** Enter the name of the departmental project office or laboratory sponsoring (*paying for*) the research and development. Include address.

13. **ABSTRACT.** Enter an abstract giving a brief and factual summary of the document indicative of the report, even though it may also appear elsewhere in the body of the technical report. If additional space is required, a continuation sheet shall be attached.

It is highly desirable that the abstract of classified reports be unclassified. Each paragraph of the abstract shall end with an indication of the military security classification of the information in the paragraph represented as (TS), (S), (C), or (U).

There is no limitation on the length of the abstract. However, the suggested length is from 150 to 225 words.

14. **KEY WORDS** Key words are technically meaningful terms or short phrases that characterize a report and may be used as index entries for cataloging the report. Key words must be selected so that no security classification is required. Identifiers, such as equipment model designation, trade name, military project code name, geographic location, may be used as key words but will be followed by an indication of technical context. The assignment of links, roles, and weights is optional.